ACS OMEGA

http://pubs.acs.org/journal/acsodf

Article

Why Should Metformin Not Be Given in Advanced Kidney Disease? Potential Leads from Computer Simulations

Visnja Kokic Males and Martina Požar*

Cite This: *ACS Omega* 2021, 6, 15382−15391

Read Online

ACCESS | Metrics & More | Article Recommendations | Supporting Information

ABSTRACT: Metformin is considered as the go-to drug in the treatment of diabetes. However, it is either prescribed in lower doses or not prescribed at all to patients with kidney problems. To find a potential explanation for this practice, we employed atomistic-level computer simulations to simulate the transport of metformin through multidrug and toxin extrusion 1 (MATE1), a protein known to play a key role in the expulsion of metformin into urine. Herein, we examine the hydrogen bonding between MATE1 and one or more metformin molecules. The simulation results indicate that metformin continuously forms and breaks off hydrogen bonds with MATE1 residues. However, the mean hydrogen bond lifetimes increase for an order of magnitude when three metformin molecules are inserted instead of one. This new insight into the metformin transport process may provide the molecular foundation behind the clinical practice of not prescribing metformin to kidney disease patients.

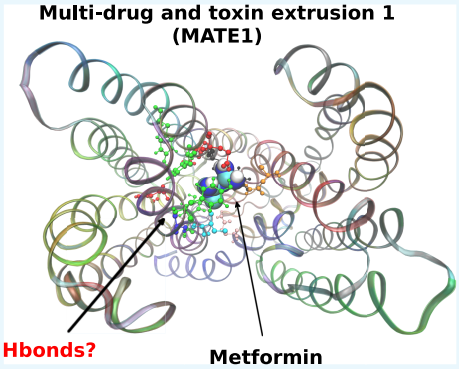

INTRODUCTION

Even after half a century of use and experience, metformin is still the gold standard in the treatment of diabetes,[1,2] despite the discovery of numerous new antidiabetic drugs. Metformin has a multitude of advantages for the patient: it is inexpensive, safe, and available in an immediate release or as an extended release form that can be given orally once or twice daily.[1,2] Metformin is not only the go-to therapy in glucose control,[3] but it also has beneficial effects on weight gain[4] and cardiovascular mortality.[5−7]

In addition to its antidiabetic effects, metformin has shown numerous pleiotropic effects.[8−10] Studies demonstrated decreased risk of the occurrence of various types of cancers, especially pancreas cancer, colon cancer, and hepatocellular carcinoma.[11−13] This observation was also confirmed by the results of many meta-analyses.[14−16] Metformin is also garnering attention for its potential in treating polycystic ovary syndrome.[9,17]

However, experience has shown that metformin does not work for every patient and some may experience unwanted side effects, like abdominal discomfort, bloating, and diarrhea.[1] Moreover, serious adverse events, such as lactic acidosis, have been linked with very high circulating levels of metformin.[18] Since the drug is cleared by renal filtration, this complication is known to occur in the cases of either overdose or acute renal failure. According to the FDA Drug Safety Communication from 2017, metformin may be safely used in patients with reduced estimated glomerular filtration rates (eGFR), where eGFR $\geq$ 30 mL/min/1.73 m^2. However, metformin is contraindicated in patients with eGFR < 30 mL/min/1.7 m^2.[19] From the point of view of the physician prescribing the drug, it is very important to determine the maximum optimal daily dose of the drug, which is often unnecessarily and unreasonably underdosed, leading to poorer antihyperglycemic and anti-inflammatory effects. Yet, the physician must be mindful of patients that exhibit some forms of kidney disease. To understand why metformin has such an effect on patients with advanced kidney disease, we must elucidate the mechanism of metformin expulsion from the body, which has been given less attention in the literature.

Due to its wealth of hydrogen-bonding functional groups, metformin has low lipid solubility and requires transporters to get to its target destinations.[20] The two families of transporters mentioned in this regard are organic cation transporters (OCTs)[21] and multidrug and toxin extrusion (MATE) proteins.[22] Whereas OCTs are required to transport metformin into the liver, gut, and kidneys,[20,21] the excretion of metformin into bile and urine via kidneys is controlled by MATE1.[20]

In this paper, we are focusing on MATE1 and its role in the transport and expulsion of metformin via molecular dynamics (MD) simulations. We discuss the interaction between MATE1 and metformin with the emphasis on the hydrogen bonding between the two. To our knowledge, there has not been an MD study on the transport of metformin through this

Received: March 31, 2021
Accepted: May 14, 2021
Published: June 1, 2021

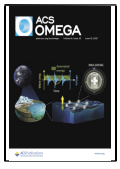

particular protein. In fact, there are a few examples of metformin simulations in the literature, either of the molecule itself or in solutions and biomacromolecular complexes.[23−27] The most recent example of a simulation study involving metformin was from Akçeşme *et al.*,[28] where the authors presented the results of metformin and human organic cation transporter (hOCT 1−3) interactions. This investigation is the most relevant to ours, as it demonstrates a stable simulation of metformin and transport proteins.

As for MATE1, the X-ray structure of the mammalian protein has not been resolved yet, but it is generally predicted as having 13 transmembrane helices (TMHs) with an extracellular C terminus.[29,30] However, the X-ray structure of its prokaryotic counterpart, NorM from *Vibrio cholerae*, is known and consists of 12 TMHs.[31] Zhang *et al.*[32] did a combined experimental and theoretical study on the mammalian MATE1 and concluded that the functional core of the protein is made up of 12 TMHs, i.e., the 13th TMH is not essential for its transport purpose. In the same study, the authors propose a theoretical model of the mammalian MATE1, obtained by homology modeling from NorM. This homology model of MATE1 was then studied via MD simulations, the results of which indicated that the modeled MATE1 was at least as stable as the NorM X-ray structure from which it is derived. The paper of Zhang *et al.* provides the foundation for the MATE1 structure in this current work.

RESULTS AND DISCUSSION

The detailed simulation protocol and force field information are contained in the Methods section. We started from the theoretical structure of MATE1 embedded in a model membrane containing 119 molecules of dipalmitoylphosphatidylcholine (DPPC). This system was then surrounded by water molecules that mimic both the extracellular space and the cytoplasm. The initial system is depicted in Figure 1, with the protein represented with ribbons, DPPC with gray lines, and water with cyan lines.

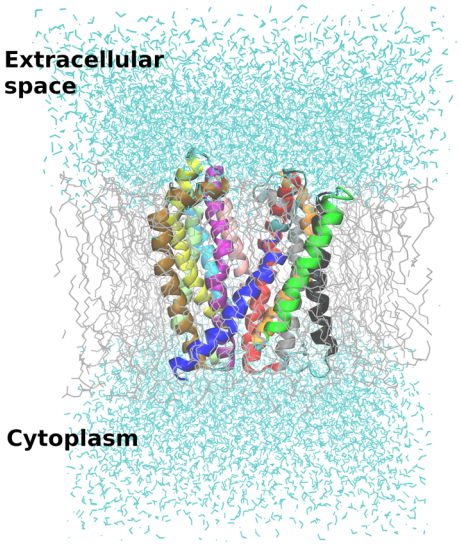

Figure 1. MATE1 proteins (ribbons) embedded into a DPPC bilayer (gray lines) and surrounded by water molecules (cyan lines). The MATE1 TMHs are color-coded from the N terminus as follows: 1, blue; 2, red; 3, gray; 4, orange; 5, green; 6, black; 7, pink; 8, magenta; 9, brown; 10, yellow; 11, cyan; 12, lime green.

The MATE1−DPPC−water system then underwent an equilibration run of 50 ns and a production run of 20 ns. The latter run was used to calculate the root-mean-square displacement (RMSD) and the radius of gyration (R_g) of the backbone of MATE1. The temporal evolution of both quantities is presented in Figures S1 and S2 in the Supporting Information, Section 2. The value for RMSD increases up to 5 ns, after which it fluctuates around the average value of (0.22 ± 0.01) nm. The radius of gyration fluctuates around the average value of (2.17 ± 0.01) nm throughout the 20 ns run. The stability of the protein model during the simulation enabled us to carry out further simulations that involved inserting metformin into the existing system.

For subsequent simulations, we inserted one molecule of metformin into the pocket of MATE1. The exact position of the molecule can be seen in the leftmost panel of Figure 2 at 0 ns. Snapshots of the molecule were taken at 50, 100, and 200 ns, respectively. The images of metformin at these points in time may give the impression that the molecule is rather static. However, this impression changes when we look at the video rendered from the 200 ns trajectory, the link for which is in the Supporting Information, Section 1. The video reveals that metformin moves quite freely within MATE1 during the course of the simulation.

Since metformin is highly hydrophilic and relies on transporters to move through membranes, we assumed that hydrogen bonding (Hbonding), a very frequent mechanism of interaction between proteins and ligands[33−35] and proteins and proteins,[36−39] is involved. We turned to hydrogen bond (HB) analysis to quantify the observations from the video. The HB analysis used in this paper is a staple in the research of liquids and liquid mixtures and workers in the field have used this methodology for quantifying the hydrogen bonding process in water,[40−43] alcohols,[44] and related mixtures.[45−48] This same analysis is relevant for studying the interaction of proteins with water, for example, in protein hydration.[49,50] In this work, we primarily focus on the interaction between metformin and the protein via Hbonding.

Other interactions that involve only the protein, such as salt bridges, do occur throughout the simulation. For the sake of completeness, we have included a short discussion on them in the Supporting Information, Section 2, but the main target of our study is the Hbonding between metformin and MATE1.

First, we calculated the number of hydrogen bonds formed between metformin and MATE1 residues according to the geometric criteria of hydrogen bond formation. To account for the weakest hydrogen bonds, which, on average, have a characteristic length of 3.4 Å,[51] we chose the cutoff radius of 3.5 Å. All of these data are collected in Figure 3, with each panel representing the number of Hbonds between metformin and a residue of MATE1.

Throughout the simulation, metformin forms Hbonds with the following AA residues: Gln-49, Asn-82, Glu-273, Trp-274, Tyr-277, Glu-278, Tyr-299, Ala-302, Ile-303, Tyr-306, Glu-389, and Tyr-416. The positions of these residues, alongside metformin at 200 ns, are depicted in Figure 4.

The distributions of the number of Hbonds in Figure 3 show that metformin simultaneously forms at most one bond with Ile-303 and Tyr-416, two bonds with Gln-49, Asn-82, Tyr-277, Tyr-299, Ala-302, and Tyr-306, and three bonds with Trp-274, Glu-273, Glu-278, and Glu-389. The fact that metformin displays a heightened interaction with the glutamine residues corroborates the suggestion of Zhang *et al.*[32] that these

https://doi.org/10.1021/acsomega.1c01744
ACS Omega 2021, 6, 15382−15391

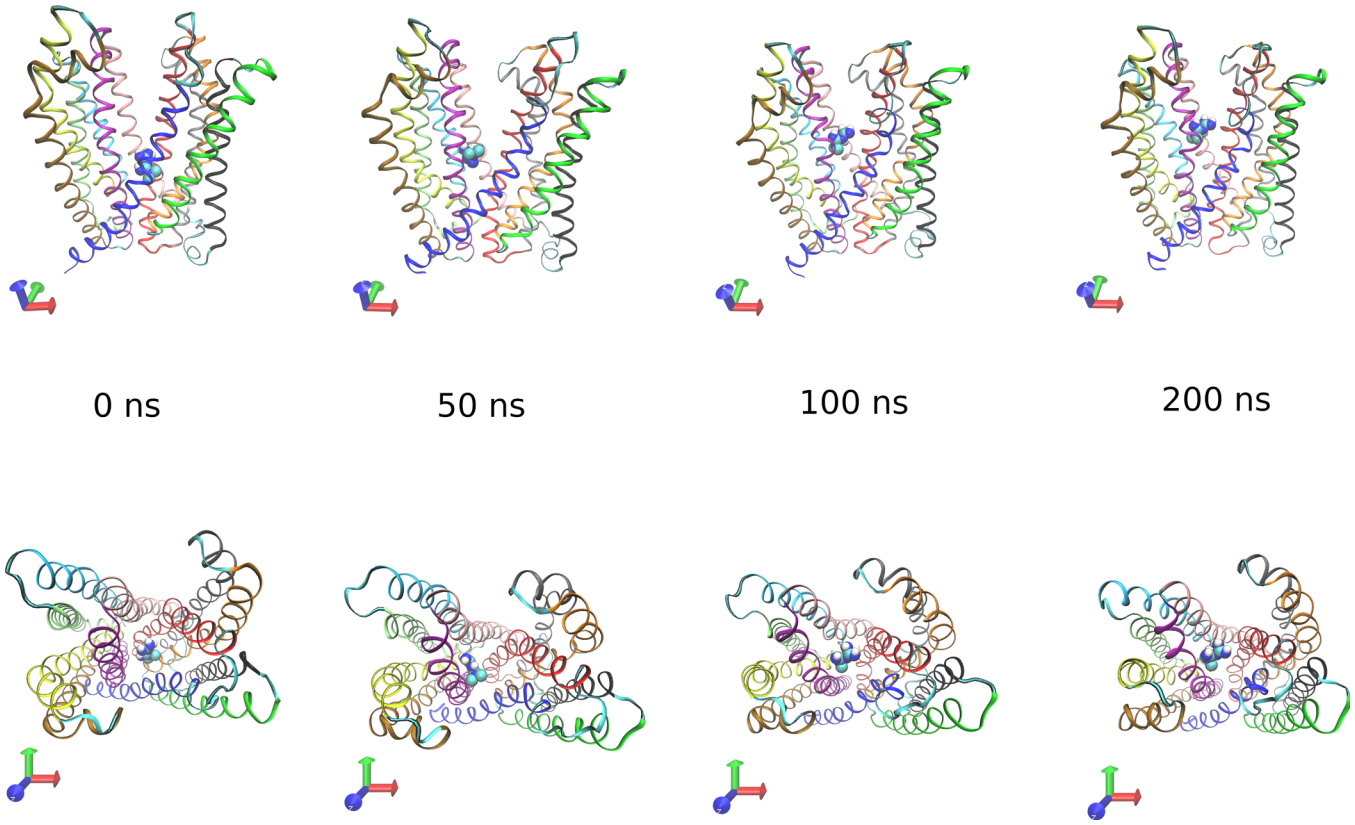

Figure 2. Temporal evolution of the passage of metformin through MATE1. The side view of the protein (top row) and its corresponding top view (bottom row) are presented for particular simulation times. The color code of the protein's TMH is the same as in Figure 1, whereas metformin's sites are as follows: nitrogen, blue; hydrogen, white; carbon, cyan.

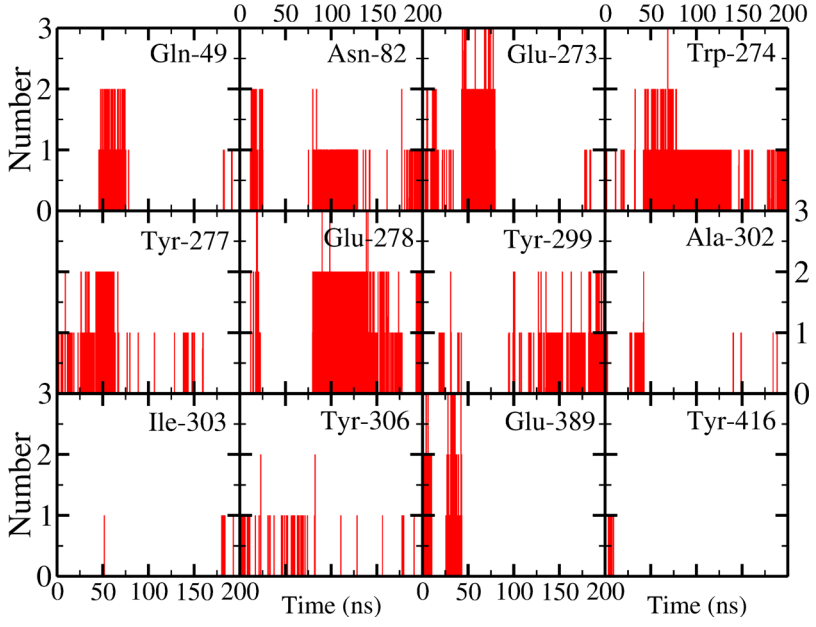

Figure 3. Number of hydrogen bonds formed by metformin and residues of MATE1 over the span of 200 ns. The residue name is given in the top right corner of each panel.

residues form the assumed translocation pathway for a substrate. Also, this result agrees with a previous experimental study by Matsumoto *et al.*,[52] which concluded that these specific residues are a part of the substrate binding site. Glu-273 is also mentioned in the study by Otsuka *et al.*[29] as being essential for transport.

To quantitatively describe the data in Figure 3, we have expressed the number of Hbonds formed between metformin and the MATE1 residues in terms of the percentages of simulation times. The four residues that contribute least significantly to the number of Hbonds are Ala-302, Ile-303, Tyr-306, and Tyr-416, which form one Hbond with metformin

https://doi.org/10.1021/acsomega.1c01744
ACS Omega 2021, 6, 15382−15391

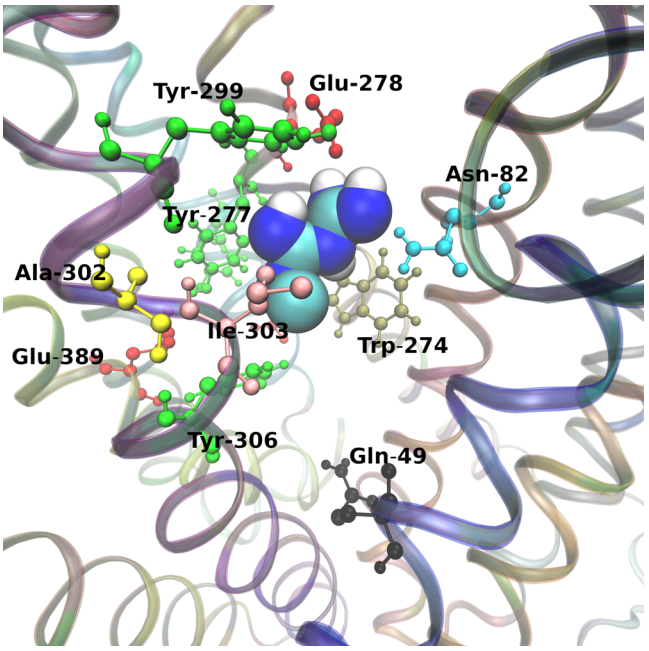

Figure 4. Snapshot of metformin with the AA residues it Hbonds with during the simulation. The name and number of the residue are featured for all visible residues.

for 0.05−0.01% of the simulation time. Ala-302 and Tyr-306 have also formed two Hbonds with metformin, but this event has happened rarely, 0.002−0.001% of the simulation time. The other eight residues show a higher frequency in Hbonding with metformin, considering either one or more bonds. Tyr-299, Tyr-277, and Glu-389 hold the middle ground, as they experience one Hbond with metformin for 3.2, 4.2, and 5% of the 200 ns simulation, respectively. The remainder of the residues spends more than 10% of time each forming one Hbond with metformin. Gln-49 has one Hbond 11% of the time, followed by Glu-273 (12.5%), Trp-274 (14.3%), Asn-82 (22.4%), and finally Glu-278 (30%).

When we consider the residues that form two Hbonds with metformin simultaneously, we see that the time percentage dwindles noticeably, with only the glutamine residues contributing more significantly. They go in ascending order: Gln-49 (0.04%), Tyr-277 (0.05%), Trp-274 (0.07%), Tyr-299 (0.09%), Asn-82 (0.1%), Glu-389 (0.4%), Glu-273 (1.4%), and Glu-389 (1.7%).

As for the residues that have presented the possibility of having three Hbonds at the same time, the percentages of the glutamine residues are the only ones of note: Glu-273 and Glu-278 (both 0.02%) and Glu-389 (0.08%).

The analysis of the hydrogen bond number points to the fact that metformin has a proclivity to bind to multiple residues at the time. However, Figure 3 might lead one to conclude that metformin spends tens of nanoseconds bound to the same AA residue once it forms an Hbond. This is not true because the number of hydrogen bonds is a static quantity, which merely counts the number of hydrogen bonds between two species at certain points in time when we collected the trajectory. To find out the dynamics of binding between metformin and MATE1, we must first calculate the probability distribution of hydrogen bond lifetimes, $P(t)$.[40,42] This is a quantity that describes the rate of survival probability for a newly generated Hbond and is described in more detail in the Methods section.

In our case, we have examined the probability distributions of Hbond lifetimes for metformin−MATE1 residue pairs, and these data are presented in Figure 5. We note that each curve is

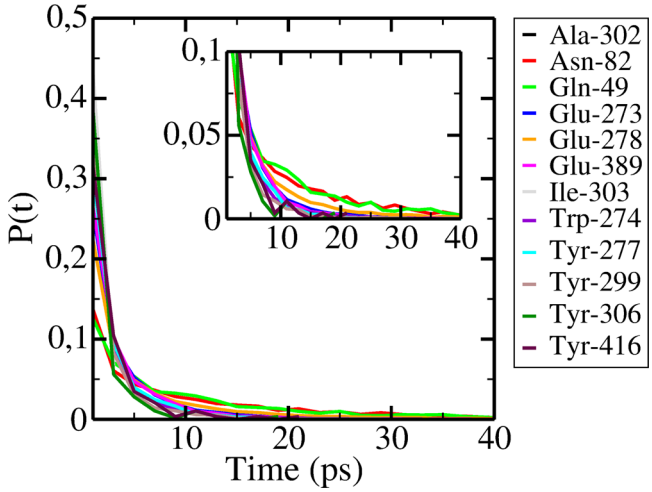

Figure 5. Probability distributions of Hbond lifetimes for AA residue−metformin. The color code for each residue is given in the figure legend.

monotonously decaying, which is even more visible in the magnified inset of Figure 5. This means that the hydrogen bonding between metformin and the MATE1 residue always follows the same trend, with the Hbond starting at one point in time and then gradually tapering off to 0 in the time span of 10 to 40 ps.

However, to obtain the numerical value known as the mean hydrogen bond lifetime $\langle\tau\rangle$, we need to do a temporal integral of the product of $P(t)$ and t[42] (also described in more detail in the Methods section). Our calculations of the mean hydrogen bond lifetimes for each metformin−MATE1 residue pair are provided in Table 1. Asn-82 has the longest mean Hbond

Table 1. Mean Hydrogen Bond Lifetimes $\langle\tau\rangle$ between Metformin and Specific MATE1 Residues

residue	$\langle\tau\rangle$ [ps]	residue	$\langle\tau\rangle$ [ps]
Ala-302	1.00	Ile-303	1.27
Asn-82	13.30	Trp-274	3.02
Gln-49	11.49	Tyr-277	2.80
Glu-273	4.05	Tyr-299	2.77
Glu-278	6.13	Tyr-306	2.02
Glu-389	3.62	Tyr-416	2.54

lifetime of 13.3 ps, followed by Gln-49, which has a $\langle\tau\rangle$ of 11.49 ps. The glutamine residues have Hbond lifetimes of 6.13, 4.05, and 3.62 ps. For the other seven residues, the Hbond lifetimes range from 3.02 to 1 ps.

The numbers in Table 1 indicate that metformin's Hbond formation with individual MATE1 residues is a short process that lasts picoseconds. Thus, metformin continuously "clicks on" and "clicks off" Hbonds with different residues; however, it stays in the vicinity of certain residues for tens of nanoseconds, continuously forming and breaking Hbonds with residues that are in the assumed translocation pathway. This explanation accounts for the jerky motion of metformin in the Supporting Information video.

https://doi.org/10.1021/acsomega.1c01744
ACS Omega 2021, 6, 15382−15391

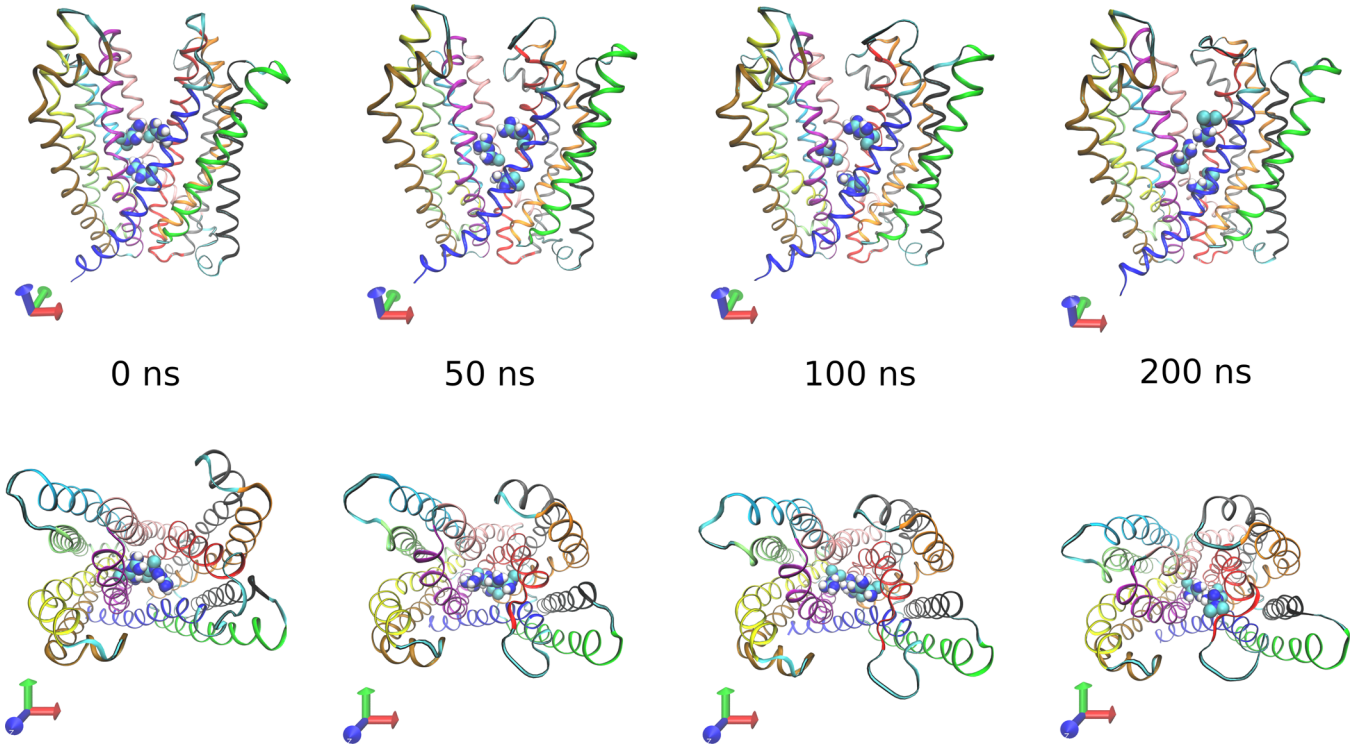

Figure 6. Temporal evolution of the passage of three metformin molecules through MATE1. The side view of the protein (top row) and corresponding top view (bottom row) are presented for a particular simulation time. The color code is the same as in Figure 2.

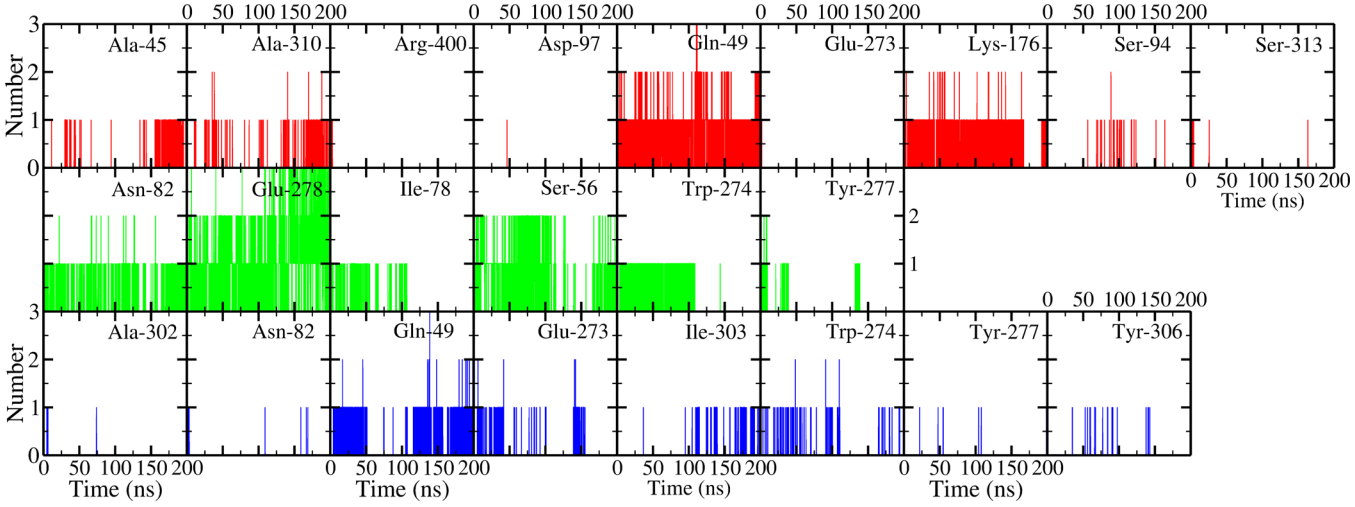

Figure 7. Number of hydrogen bonds formed by three metformin molecules and residues of MATE1 over the span of 200 ns. Metformin molecule 1 (red) is in the top row, molecule 2 (green) is in the middle row, and molecule 3 (blue) is in the bottom row. The residue name is given in the top right corner of each panel.

To put the calculated numbers into perspective, we have also determined the mean hydrogen bond lifetime for other constituents of the system. Water can Hbond with metformin but also with MATE1 residues and other water molecules. The water−water combination has a mean Hbond lifetime of 0.27 ps, 2.2 ps for water−metformin, and 46.8 ps for water−MATE1 (with the MATE1 residues on average).

During the 200 ns simulation, metformin has not passed through MATE1, but we speculate that this process requires more computational time, perhaps in the range of microseconds. It is also possible that the passage of metformin through MATE1 is modulated by the number of metformin molecules present. With more metformin molecules in the protein, there are a larger number of Hbond donors and acceptors that may compete for binding with residues in the presumed translocation pathway. This may affect the quantities related to hydrogen bonding and, consequentially, the time necessary for metformin to be excreted.

To examine that notion, we returned to the initial MATE1−DPPC−water system and inserted three metformin molecules into the cleft of MATE1. Figure 6 gives us snapshots of the system during 200 ns of the simulation. Just like in Figure 2, we present the configurations of the system at 0, 50, 100, and 200 ns. The motion of the molecules can be examined further in

https://doi.org/10.1021/acsomega.1c01744
ACS Omega 2021, 6, 15382−15391

the video available on the link in the Supporting Information, Section 1, just like in the case of one metformin in the cleft. Similarly, we performed the same type of Hbond analysis as for the system with one metformin. The results of the Hbond number for each metformin molecule are shown in Figure 7. To get a better grasp of the labeling of each metformin, we provide Figure 8.

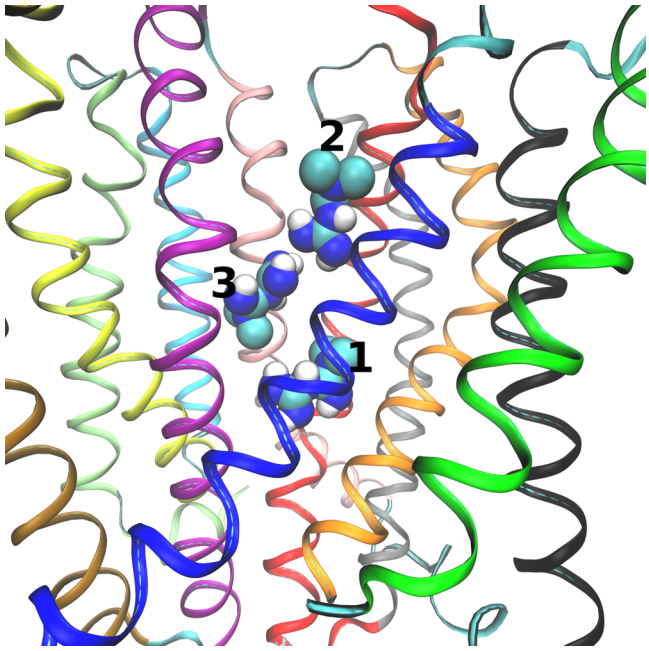

Figure 8. Three metformin molecules in the MATE1 cleft, labeled (1/2/3), as they were subsequently referenced.

The first metformin molecule (top row of Figure 7, in red) formed Hbonds with nine MATE1 AA residues during the simulation. For the most part, it formed one Hbond with the residues, out of which 58.7% of the time with Gln-49 and 40.6% with Lys-176. The second metformin (middle row of Figure 7, in green) bonded with six AA residues, most notably one Hbond with Glu-273 (57% of the time), Ser-56 (47% of the time), Trp-274 (31% of the time), and Asn-82 (13.4% of the time). The second metformin also significantly forms multiple Hbonds, two bonds with Glu-278 (22% of the time) and Ser-56 (3.5% of the time) and even three bonds with Glu-278 (3.7% of the time). The third metformin, on the other hand, only forms one Hbond for notable amounts of time: with Gln-49 for 22.7% of the 200 ns simulation and Glu-273 for 5.8%. The distributions of the number of Hbonds over different AA residues underscore the activity and importance that certain residues like Glu-273, Glu-278, and Gln-49 have in the pocket of MATE1.

Since the probability distributions of hydrogen bond lifetimes for each metformin−residue follow the same trend as in Figure 5, we only present the calculated mean hydrogen bond lifetimes in Table 2. All three metformin molecules experience mean Hbond lifetimes in the range of tens, and for certain AA residues, hundreds of picoseconds, which is a significant increase in comparison to the situation with only one metformin (Table 1). This is particularly prominent for the second metformin molecule, which has a mean Hbond lifetime of over 100 ps for two residues, Ser-56 and Trp-274. It seems that the increased number of metformins in the MATE1 cleft slows down the Hbond dynamics of all the molecules with the protein residues. The metformins still "click on" and "click off" Hbonds with the AA residues, but those processes take, on an order of magnitude, more time than in the case of a single metformin molecule.

Table 2. Mean Hydrogen Bond Lifetimes $\langle\tau\rangle$ between Each Metformin and Specific MATE1 Residues

metformin 1		metformin 2		metformin 3	
residue	$\langle\tau\rangle$ [ps]	residue	$\langle\tau\rangle$ [ps]	residue	$\langle\tau\rangle$ [ps]
Ala-45	42.50	Asn-82	49.41	Ala-302	20.00
Ala-310	26.43	Glu-278	94.87	Asn-82	81.05
Arg-400	23.64	Ile-78	25.03	Gln-49	51.56
Asp-97	20.00	Ser-56	159.93	Glu-273	43.35
Gln-49	101.23	Trp-274	104.02	Ile-303	30.59
Glu-273	33.33	Tyr-277	54.95	Trp-274	21.90
Lys-176	71.24			Tyr-277	20.00
Ser-94	27.41			Tyr-306	24.00
Ser-313	42.22				

With the metformin molecules in close proximity, it is important to examine if there are any Hbond interactions between them. We calculated the number of Hbonds between all the possible pairs of metformins. This information is contained in the Supporting Information, Section 2, Figure S4. Throughout the simulation, metformin molecules 1 and 2 do not form hydrogen bonds at all, whereas the number of Hbonds between the two other pairs is almost entirely 1. In addition to that, the molecules form Hbonds for only 0.13 and 0.07% of the total simulation time. As for the mean hydrogen bond lifetime, we calculated it to be 1.04 and 1.05 ps for the metformin 1−3 pair and metformin 2−3 pair, respectively. The simulation points to the idea that when multiple metformin molecules are within MATE1, the molecules will interact more with the protein residues than with other metformin molecules and these bonds will have a longer mean lifetime. This trend is also present when we consider water molecules, the mean hydrogen lifetimes of which align with the numbers presented for the simulation with only one metformin. This information is very interesting from the clinical aspect of prescribing the drug. The longer-lasting Hbonds between multiple metformins and MATE1 can mean that more time is necessary for the expulsion of more metformin molecules. This sheds new light on the fact that the implementation of metformin therapy to more advanced stages of chronic kidney disease (eGFR < 30 mL/min/1.73 m^2[19]) is potentially dangerous.

SUMMARY

In summary, the present study showed that computer simulations reveal a wealth of information about the interactions of metformin and MATE1 on the atomistic level of detail. First, we have further confirmed that the theoretical model of MATE1, first presented by Zhang *et al.*,[32] is stable throughout MD simulations of even longer duration than in the original study, thus making it an excellent basis for studying the interactions with small organic molecules. This enabled us to perform novel simulations of MATE1 with one or more metformin molecules inserted in its pocket and analyze the results with particular emphasis on the hydrogen bonding between metformin and the protein.

In the case of one metformin, the results indicate that metformin continually forms and breaks off hydrogen bonds with MATE1 residues, the mean hydrogen bond lifetime being

https://doi.org/10.1021/acsomega.1c01744
ACS Omega 2021, 6, 15382−15391

from 1 to 13.3 ps. However, metformin tends to hydrogen-bond to specific MATE1 residues, among which are Glu-278, Asn-82, Trp-274, Glu-273, Gln-49, Glu-389, Tyr-277, and Try-299. Metformin's heightened bonding preference toward glutamine residues was previously noted by Matsumoto *et al.*,[52] so our results confirm that these residues play a part in the presumed translocation pathway in MATE1.

Inserting more metformin molecules in the cleft of MATE1 slows down the dynamic of hydrogen bonding between metformin and the AA residues, as witnessed by the mean hydrogen bond lifetime that increased to tens and even hundreds of picoseconds in some cases. The metformin molecules bond more to the protein than to themselves, with the choice of AA residues for bonding influenced by the available space in the pocket, i.e., the other metformin molecules hinder the mobility in the pocket. If metformins hydrogen-bond among themselves, those bonds are short-lived, the mean lifetime being hardly more than 1 ps. However, the picture of constant hydrogen bond formation and destruction still persists, despite the slowdown in the hydrogen bond dynamics.

Since the metformin molecules did not pass through MATE1 during our 200 ns simulations, we speculate that more simulation time is necessary to observe that process, possibly in the range of microseconds. Further studies are required to examine that point. Nonetheless, this present study gives new insight into the interaction between metformin and MATE1, emphasizing the role of hydrogen bonding. It may serve as a stepping stone toward understanding the excretion mechanism of the versatile and important drug that is metformin.

METHODS

Simulation Details. The creation of the systems and subsequent simulations were performed in the Gromacs program package, version 5.1.4.[53] The structure of the multidrug and toxin extrusion protein 1 (MATE1) was embedded into a pre-equilibrated DPPC bilayer (containing 119 DPPC molecules), and the rest of the simulation box was filled with water molecules. To retain the electroneutrality of the system, one chlorine ion was added into the water surrounding the MATE1−DPPC bilayer structure.

This system was then energy-minimized, followed by a 1 ns NVT equilibration and a 50 ns NpT equilibration. Since DPPC has a phase transition at 315 K,[54] the temperature of choice for simulating a system with this bilayer has to be above that value. To get the system to the desired temperature of 323 K, the v-rescale thermostat[55] was used in the NVT stage of equilibration, whereas the Nose−Hoover thermostat[56,57] was used during the NpT equilibration. The Parrinello−Rahman barostat[58,59] was employed to keep the pressure at 1 bar. In both algorithms, the time constant was set to 0.5 ps. The time step for equations of motions was 2 fs. The long-range electrostatics were handled with the particle mesh Ewald (PME) method.[60]

After the equilibration step, one metformin molecule was inserted in the simulation box, in the MATE1 pocket. A production run of 200 ns was performed, with the temperature of 323 K and the pressure of 1 bar being regulated by the Nose−Hoover thermostat[56,57] and the Parrinello−Rahman barostat,[58,59] respectively. The other specifications are the same as in the NpT equilibration step. The trajectories of the atoms were collected every 2 ps.

A second system with three metformin molecules in the MATE1 cleft was created. The specifications of the production run are the same as in the case with one metformin molecule.

The Gromos 54a7 force field[61] was used for the MATE1 protein, the DPPC bilayer, and metformin. The details about the metformin model are provided in the Supporting Information, Section 3. The theoretical model of multidrug and toxin extrusion protein 1 (MATE1) was taken from the Swiss model repository (Q96FL8 (S47A1_HUMAN)).[62] This model was obtained via homology modeling from the X-ray crystal structure of a MATE family protein derived from *Camelina sativa* at 2.3 Å (PDB code 5YCK).[63] In the Supporting Information, Section 3, we discuss the salient points of the bioinformatic analysis and compare the MATE1 model featured in this paper with the NorM model from Zhang *et al.*[32]

The paper of Kukol[64] was useful for modeling the DPPC bilayer. The structure of metformin originates from the Automated Topology Builder.[64−67] For water, we used the SPC/e model.[68] The snapshots and videos of the MATE1−DPPC−water system with one and three metformin molecules, respectively, were created with VMD version 1.9.1.[69,70]

Theoretical Details. The root-mean-square displacement (RMSD) of a structure is calculated as[62,71]

$$\mathrm{RMSD}(t) = \left[\frac{1}{M}\sum_{i=1}^{N} m_i |r_i(t) - r_i^{\mathrm{ref}}|^2\right]^{1/2}$$

where $M = \Sigma_i m_i$ with m_i being the mass of atom i, $r_i(t)$ is the position of atom i at time t, and r_i^{ref} is the position of atom i in a reference structure. Hence, RMSD is a quantity that tells us the average distance between two structures.

The radius of gyration (R_g) is calculated as[71]

$$R_g = \left(\frac{\sum_i |r_i|^2 m_i}{\sum_i m_i}\right)^{1/2}$$

where m_i is the mass of atom i, and r_i is the position of atom i in relation to the center of mass of the molecule.

The number of hydrogen bonds in time is calculated based on geometric criteria: the distance of donor−acceptor (which we took as 3.5 Å) and the angle between hydrogen−donor−acceptor (30°).

The probability distribution of hydrogen bond lifetimes, $P(t)$, is calculated as[40,42]

$$P(t) = -\frac{\mathrm{d}s(t)}{\mathrm{d}t}$$

where $s(t)$ is the survival probability for a newly generated hydrogen bond.

The probability distribution of hydrogen bond lifetimes, $P(t)$, is used to calculate the mean hydrogen bond lifetime $\langle\tau\rangle$:[42]

$$\langle\tau\rangle = \int_0^\infty P(t)\cdot t\cdot \mathrm{d}t$$

The salt bridges for MATE1, which are featured in the Supporting Information, Section 2, are calculated based on geometric criteria. The salt bridge exists between any of the oxygen atoms of acidic residues and the nitrogen atoms of basic residues within the standard 3.2 Å cutoff distance.[72,73]

https://doi.org/10.1021/acsomega.1c01744
ACS Omega 2021, 6, 15382−15391

■ ASSOCIATED CONTENT

Supporting Information

The Supporting Information is available free of charge at https://pubs.acs.org/doi/10.1021/acsomega.1c01744.

Video links, additional results of the MATE1−DPPC−water system (RMSD and the radius of gyration), discussion about the salt bridges occurring in MATE1, additional results for the MATE1−DPPC−water system with three metformins (number of Hbonds), details about the metformin model, and bioinformatic analysis of the MATE1 model (PDF)

■ AUTHOR INFORMATION

Corresponding Author

Martina Požar − *Faculty of Science, University of Split, 21000 Split, Croatia;* orcid.org/0000-0001-6300-2204; Email: marpoz@pmfst.hr

Author

Visnja Kokic Males − *University Department for Health Studies, University of Split, 21000 Split, Croatia*

Complete contact information is available at: https://pubs.acs.org/10.1021/acsomega.1c01744

Author Contributions

The manuscript was written through contributions of both authors. Both authors have given approval to the final version of the manuscript.

Funding

This work has been supported by the Croatian Science Foundation under the project UIP-2017-05-1863 "Dynamics in micro-segregated systems".

Notes

The authors declare no competing financial interest.

■ ACKNOWLEDGMENTS

We gratefully acknowledge the computational resources provided by the Center for Advanced Computing and Modeling, University of Rijeka (HPC Bura).

■ ABBREVIATIONS

eGFR, estimated glomerular filtration rates; OCT, organic cation transporters; MATE1, multidrug and toxin extrusion protein 1; TMHs, transmembrane helices; MD, molecular dynamics; DPPC, dipalmitoylphosphatidylcholine; Hbond, hydrogen bond; AA, amino acid

■ REFERENCES

(1) American Diabetes Association. 9. Pharmacologic Approaches to Glycemic Treatment. *Diabetes Care* **2020**, *43*, S98−S110.

(2) Rodbard, H. W.; Jellinger, P. S.; Davidson, J. A.; Einhorn, D.; Garber, A. J.; Grunberger, G.; Handelsman, Y.; Horton, E. S.; Lebovitz, H.; Levy, P.; Moghissi, E. S.; Schwartz, S. S. Statement by an American Association of Clinical Endocrinologists/American College of Endocrinology Consensus Panel on Type 2 Diabetes Mellitus: An Algorithm for Glycemic Control. *Endocr. Pract.* **2009**, *15*, 540−559.

(3) Knowler, W. C.; Barrett-Connor, E.; Fowler, S. E.; Hamman, R. F.; Lachin, J. M.; Walker, E. A.; Nathan, D. M. Diabetes Prevention Program Research Group. Reduction in the Incidence of Type 2 Diabetes with Lifestyle Intervention or Metformin. *N. Engl. J. Med.* **2002**, *346*, 393−403.

(4) Effect of Intensive Blood-Glucose Control with Metformin on Complications in Overweight Patients with Type 2 Diabetes (UKPDS 34). *Lancet* **1998**, *352* (), 854−865, DOI: 10.1016/S0140-6736(98)07037-8.

(5) Holman, R. R.; Paul, S. K.; Bethel, M. A.; Matthews, D. R.; Neil, H. A. W. 10-Year Follow-up of Intensive Glucose Control in Type 2 Diabetes. *N. Engl. J. Med.* **2008**, *359*, 1577−1589.

(6) Maruthur, N. M.; Tseng, E.; Hutfless, S.; Wilson, L. M.; Suarez-Cuervo, C.; Berger, Z.; Chu, Y.; Iyoha, E.; Segal, J. B.; Bolen, S. Diabetes Medications as Monotherapy or Metformin-Based Combination Therapy for Type 2 Diabetes: A Systematic Review and Meta-Analysis. *Ann. Intern. Med.* **2016**, *164*, 740−751.

(7) Zhang, Y.; Hu, C.; Hong, J.; Zeng, J.; Lai, S.; Lv, A.; Su, Q.; Dong, Y.; Zhou, Z.; Tang, W.; Zhao, J.; Cui, L.; Zou, D.; Wang, D.; Li, H.; Liu, C.; Wu, G.; Shen, J.; Zhu, D.; Wang, W.; Shen, W.; Ning, G.; Xu, G. Lipid Profiling Reveals Different Therapeutic Effects of Metformin and Glipizide in Patients with Type 2 Diabetes and Coronary Artery Disease. *Diabetes Care* **2014**, *37*, 2804−2812.

(8) Foretz, M.; Guigas, B.; Viollet, B. Understanding the Glucoregulatory Mechanisms of Metformin in Type 2 Diabetes Mellitus. *Nat. Rev. Endocrinol.* **2019**, *15*, 569−589.

(9) Viollet, B.; Guigas, B.; Sanz Garcia, N.; Leclerc, J.; Foretz, M.; Andreelli, F. Cellular and Molecular Mechanisms of Metformin: An Overview. *Clin. Sci.* **2012**, *122*, 253−270.

(10) Prattichizzo, F.; Giuliani, A.; Mensà, E.; Sabbatinelli, J.; De Nigris, V.; Rippo, M. R.; La Sala, L.; Procopio, A. D.; Olivieri, F.; Ceriello, A. Pleiotropic Effects of Metformin: Shaping the Microbiome to Manage Type 2 Diabetes and Postpone Ageing. *Ageing Res. Rev.* **2018**, *48*, 87−98.

(11) Ben Sahra, I.; Laurent, K.; Giuliano, S.; Larbret, F.; Ponzio, G.; Gounon, P.; Le Marchand-Brustel, Y.; Giorgetti-Peraldi, S.; Cormont, M.; Bertolotto, C.; Deckert, M.; Auberger, P.; Tanti, J.-F.; Bost, F. Targeting Cancer Cell Metabolism: The Combination of Metformin and 2-Deoxyglucose Induces p53-Dependent Apoptosis in Prostate Cancer Cells. *Cancer Res.* **2010**, *70*, 2465−2475.

(12) Buzzai, M.; Jones, R. G.; Amaravadi, R. K.; Lum, J. J.; DeBerardinis, R. J.; Zhao, F.; Viollet, B.; Thompson, C. B. Systemic Treatment with the Antidiabetic Drug Metformin Selectively Impairs p53-Deficient Tumor Cell Growth. *Cancer Res.* **2007**, *67*, 6745−6752.

(13) Li, D.; Yeung, S.-C. J.; Hassan, M. M.; Konopleva, M.; Abbruzzese, J. L. Antidiabetic Therapies Affect Risk of Pancreatic Cancer. *Gastroenterology* **2009**, *137*, 482−488.

(14) Kasznicki, J.; Sliwinska, A.; Drzewoski, J. Metformin in Cancer Prevention and Therapy. *Ann Transl Med* **2014**, *2*, 57.

(15) Decensi, A.; Puntoni, M.; Goodwin, P.; Cazzaniga, M.; Gennari, A.; Bonanni, B.; Gandini, S. Metformin and Cancer Risk in Diabetic Patients: A Systematic Review and Meta-Analysis. *Cancer Prev. Res.* **2010**, *3*, 1451−1461.

(16) Ng, C.-A. W.; Jiang, A. A.; Toh, E. M. S.; Ng, C. H.; Ong, Z. H.; Peng, S.; Tham, H. Y.; Sundar, R.; Chong, C. S.; Khoo, C. M. Metformin and Colorectal Cancer: A Systematic Review, Meta-Analysis and Meta-Regression. *Int. J. Colorectal Dis.* **2020**, *35*, 1501−1512.

(17) Morley, L. C.; Tang, T.; Yasmin, E.; Norman, R. J.; Balen, A. H. Insulin-Sensitising Drugs (metformin, Rosiglitazone, Pioglitazone, D-Chiro-Inositol) for Women with Polycystic Ovary Syndrome, Oligo Amenorrhoea and Subfertility. *Cochrane Database Syst. Rev.* **2017**, *11*, CD003053.

(18) Salber, G. J.; Wang, Y.-B.; Lynch, J. T.; Pasquale, K. M.; Rajan, T. V.; Stevens, R. G.; Grady, J. J.; Kenny, A. M. Metformin Use in Practice: Compliance With Guidelines for Patients With Diabetes and Preserved Renal Function. *Clin. Diabetes* **2017**, *35*, 154−161.

(19) *Center for Drug Evaluation; Research. Warning use metformin in certain patients with reduced kidney function*https://www.fda.gov/drugs/drug-safety-and-availability/fda-drug-safety-communication-fda-revises-warnings-regarding-use-diabetes-medicine-metformin-certain (accessed Mar 20, 2021).

(20) Graham, G. G.; Punt, J.; Arora, M.; Day, R. O.; Doogue, M. P.; Duong, J. K.; Furlong, T. J.; Greenfield, J. R.; Greenup, L. C.; Kirkpatrick, C. M.; Ray, J. E.; Timmins, P.; Williams, K. M. Clinical

Pharmacokinetics of Metformin. *Clin. Pharmacokinet.* **2011**, *50*, 81−98.
(21) Nies, A. T.; Hofmann, U.; Resch, C.; Schaeffeler, E.; Rius, M.; Schwab, M. Proton Pump Inhibitors Inhibit Metformin Uptake by Organic Cation Transporters (OCTs). *PLoS One* **2011**, *6*, No. e22163.
(22) Tanihara, Y.; Masuda, S.; Sato, T.; Katsura, T.; Ogawa, O.; Inui, K.-I. Substrate Specificity of MATE1 and MATE2-K, Human Multidrug and Toxin extrusions/H(+)-Organic Cation Antiporters. *Biochem. Pharmacol.* **2007**, *74*, 359−371.
(23) Mondal, S.; Samajdar, R. N.; Mukherjee, S.; Bhattacharyya, A. J.; Bagchi, B. Unique Features of Metformin: A Combined Experimental, Theoretical, and Simulation Study of Its Structure, Dynamics, and Interaction Energetics with DNA Grooves. *J. Phys. Chem. B* **2018**, *122*, 2227−2242.
(24) Rahnama, E.; Mahmoodian-Moghaddam, M.; Khorsand-Ahmadi, S.; Saberi, M. R.; Chamani, J. Binding Site Identification of Metformin to Human Serum Albumin and Glycated Human Serum Albumin by Spectroscopic and Molecular Modeling Techniques: A Comparison Study. *J. Biomol. Struct. Dyn.* **2015**, *33*, 513−533.
(25) Sahihi, M.; Ghayeb, Y. Binding of Biguanides to β-Lactoglobulin: Molecular-Docking and Molecular Dynamics Simulation Studies. *Chem. Pap.* **2014**, DOI: 10.2478/s11696-014-0598-7.
(26) Xiao, H.; Zhang, J.; Xu, Z.; Feng, Y.; Zhang, M.; Liu, J.; Chen, R.; Shen, J.; Wu, J.; Lu, Z.; Fang, X.; Li, J.; Zhang, Y. Metformin Is a Novel Suppressor for Transforming Growth Factor (TGF)-β1. *Sci. Rep.* **2016**, *6*, 28597.
(27) Fakhari, S.; Nouri, A.; Jamzad, M.; Arab-Salmanabadi, S.; Falaki, F. Investigation of Inclusion Complex of Metformin into Selective Cyclic Peptides as Novel Drug Delivery System: Structure, Electronic Properties, AIM, and NBO Study via DFT. *J. Chin. Chem. Soc.* **2021**, *68*, 67−75.
(28) Akçeşme, F. B.; Besli, N.; Pena-Garcia, J.; Parez-Sanchez, H. Assessment of Interaction of Human OCT 1-3 Proteins and Metformin Using Silico Analyses. *Acta Chim. Slov.* **2020**, *67*, 1202−1215.
(29) Otsuka, M.; Matsumoto, T.; Morimoto, R.; Arioka, S.; Omote, H.; Moriyama, Y. A Human Transporter Protein That Mediates the Final Excretion Step for Toxic Organic Cations. *Proc. Natl. Acad. Sci. U. S. A.* **2005**, *102*, 17923−17928.
(30) Motohashi, H.; Inui, K.-I. Multidrug and Toxin Extrusion Family SLC47: Physiological, Pharmacokinetic and Toxicokinetic Importance of MATE1 and MATE2-K. *Mol. Aspects Med.* **2013**, *34*, 661−668.
(31) He, X.; Szewczyk, P.; Karyakin, A.; Evin, M.; Hong, W.-X.; Zhang, Q.; Chang, G. Structure of a Cation-Bound Multidrug and Toxic Compound Extrusion Transporter. *Nature* **2010**, *467*, 991−994.
(32) Zhang, X.; He, X.; Baker, J.; Tama, F.; Chang, G.; Wright, S. H. Twelve Transmembrane Helices Form the Functional Core of Mammalian MATE1 (multidrug and Toxin Extruder 1) Protein. *J. Biol. Chem.* **2012**, *287*, 27971−27982.
(33) Chen, D.; Oezguen, N.; Urvil, P.; Ferguson, C.; Dann, S. M.; Savidge, T. C. Regulation of Protein-Ligand Binding Affinity by Hydrogen Bond Pairing. *Sci. Adv.* **2016**, *2*, No. e1501240.
(34) Itoh, Y.; Nakashima, Y.; Tsukamoto, S.; Kurohara, T.; Suzuki, M.; Sakae, Y.; Oda, M.; Okamoto, Y.; Suzuki, T. N-C-H···O Hydrogen Bonds in Protein-Ligand Complexes. *Sci. Rep.* **2019**, *9*, 767.
(35) Meelua, W.; Wanjai, T.; Thinkumrob, N.; Oláh, J.; Mujika, J. I.; Ketudat-Cairns, J. R.; Hannongbua, S.; Jitonnom, J. Active Site Dynamics and Catalytic Mechanism in Arabinan Hydrolysis Catalyzed by GH43 Endo-Arabinanase from QM/MM Molecular Dynamics Simulation and Potential Energy Surface. *J. Biomol. Struct. Dyn.* **2021**, 1−11.
(36) Myers, J. K.; Pace, C. N. Hydrogen Bonding Stabilizes Globular Proteins. *Biophys. J.* **1996**, *71*, 2033−2039.
(37) Jitonnom, J.; Mulholland, A. J. Insights into Conformational Changes of Procarboxypeptidase A and B from Simulations: A Plausible Explanation for Different Intrinsic Activity. *Theor. Chem. Acc.* **2012**, *131*, 1224.
(38) Jitonnom, J.; Sontag, C. Comparative Study on Activation Mechanism of Carboxypeptidase A1, A2 and B: First Insights from Steered Molecular Dynamics Simulations. *J. Mol. Graphics Modell.* **2012**, *38*, 298−303.
(39) Newberry, R. W.; Raines, R. T. A Prevalent Intraresidue Hydrogen Bond Stabilizes Proteins. *Nat. Chem. Biol.* **2016**, *12*, 1084−1088.
(40) Luzar, A.; Chandler, D. Application of the Reactive Flux Formalism to Study Water Hydrogen Bond Dynamics. In *Hydrogen Bond Networks*; Springer Netherlands: Dordrecht, 1994; pp. 239−246.
(41) Luzar, A.; Chandler, D. Hydrogen-Bond Kinetics in Liquid Water. *Nature* **1996**, *379*, 55−57.
(42) Luzar, A. Resolving the Hydrogen Bond Dynamics Conundrum. *J. Chem. Phys.* **2000**, *113*, 10663−10675.
(43) Sciortino, F.; Poole, P. H.; Stanley, H. E.; Havlin, S. Lifetime of the Bond Network and Gel-like Anomalies in Supercooled Water. *Phys. Rev. Lett.* **1990**, *64*, 1686−1689.
(44) Saiz, L.; Padró, J. A.; Guàrdia, E. Structure and Dynamics of Liquid Ethanol. *J. Phys. Chem. B* **1997**, *101*, 78−86.
(45) Luzar, A.; Chandler, D. Structure and Hydrogen Bond Dynamics of Water−dimethyl Sulfoxide Mixtures by Computer Simulations. *J. Chem. Phys.* **1993**, *98*, 8160−8173.
(46) Cerar, J.; Jamnik, A.; Pethes, I.; Temleitner, L.; Pusztai, L.; Tomšič, M. Structural, Rheological and Dynamic Aspects of Hydrogen-Bonding Molecular Liquids: Aqueous Solutions of Hydrotropic Tert-Butyl Alcohol. *J. Colloid Interface Sci.* **2020**, *560*, 730−742.
(47) Jukić, I.; Požar, M.; Lovrinčević, B. Comparative Analysis of Ethanol Dynamics in Aqueous and Non-Aqueous Solutions. *Phys. Chem. Chem. Phys.* **2020**, *22*, 23856−23868.
(48) Lovrinčević, B.; Požar, M.; Balić, M. Dynamics of Urea-Water Mixtures Studied by Molecular Dynamics Simulation. *J. Mol. Liq.* **2020**, *300*, 112268.
(49) Jana, B.; Pal, S.; Bagchi, B. Hydration Dynamics of Protein Molecules in Aqueous Solution: Unity among Diversity. *J. Chem. Sci.* **2012**, *124*, 317−325.
(50) Nandi, P. K.; English, N. J.; Futera, Z.; Benedetto, A. Hydrogen-Bond Dynamics at the Bio-Water Interface in Hydrated Proteins: A Molecular-Dynamics Study. *Phys. Chem. Chem. Phys.* **2016**, *19*, 318−329.
(51) Ferreira de Freitas, R.; Schapira, M. A Systematic Analysis of Atomic Protein-Ligand Interactions in the PDB. *Medchemcomm* **2017**, *8*, 1970−1981.
(52) Matsumoto, T.; Kanamoto, T.; Otsuka, M.; Omote, H.; Moriyama, Y. Role of Glutamate Residues in Substrate Recognition by Human MATE1 Polyspecific H+/organic Cation Exporter. *Am. J. Physiol. Cell Physiol.* **2008**, *294*, C1074−C1078.
(53) Pronk, S.; Páll, S.; Schulz, R.; Larsson, P.; Bjelkmar, P.; Apostolov, R.; Shirts, M. R.; Smith, J. C.; Kasson, P. M.; van der Spoel, D.; Hess, B.; Lindahl, E. GROMACS 4.5: A High-Throughput and Highly Parallel Open Source Molecular Simulation Toolkit. *Bioinformatics* **2013**, *29*, 845−854.
(54) Nagle, J. F. Area/lipid of Bilayers from NMR. *Biophys. J.* **1993**, *64*, 1476−1481.
(55) Bussi, G.; Donadio, D.; Parrinello, M. Canonical Sampling through Velocity Rescaling. *J. Chem. Phys.* **2007**, *126*, No. 014101.
(56) Nosé, S. A Molecular Dynamics Method for Simulations in the Canonical Ensemble. *Mol. Phys.* **1984**, *52*, 255−268.
(57) Hoover, W. G. Canonical Dynamics: Equilibrium Phase-Space Distributions. *Phys. Rev. A* **1985**, *31*, 1695−1697.
(58) Parrinello, M.; Rahman, A. Crystal Structure and Pair Potentials: A Molecular-Dynamics Study. *Phys. Rev. Lett.* **1980**, *45*, 1196−1199.
(59) Parrinello, M.; Rahman, A. Polymorphic Transitions in Single Crystals: A New Molecular Dynamics Method. *J. Appl. Phys.* **1981**, *52*, 7182−7190.

https://doi.org/10.1021/acsomega.1c01744
ACS Omega 2021, 6, 15382−15391

(60) Darden, T.; York, D.; Pedersen, L. Particle Mesh Ewald: AnN·log(N) Method for Ewald Sums in Large Systems. *J. Chem. Phys.* **1993**, *98*, 10089−10092.
(61) Schmid, N.; Eichenberger, A. P.; Choutko, A.; Riniker, S.; Winger, M.; Mark, A. E.; van Gunsteren, W. F. Definition and Testing of the GROMOS Force-Field Versions 54A7 and 54B7. *Eur. Biophys. J.* **2011**, *40*, 843−856.
(62) Bienert, S.; Waterhouse, A.; de Beer, T. A. P.; Tauriello, G.; Studer, G.; Bordoli, L.; Schwede, T. The SWISS-MODEL Repository—new Features and Functionality. *Nucleic Acids Res.* **2017**, *45*, D313−D319.
(63) Tanaka, Y.; Iwaki, S.; Tsukazaki, T. Crystal Structure of a Plant Multidrug and Toxic Compound Extrusion Family Protein. *Structure* **2017**, *25*, 1455−1460.e2.
(64) Kukol, A. Lipid Models for United-Atom Molecular Dynamics Simulations of Protein. *Nat. Prec.* **2011**, DOI: 10.1038/npre.2011.5977.1.
(65) Malde, A. K.; Zuo, L.; Breeze, M.; Stroet, M.; Poger, D.; Nair, P. C.; Oostenbrink, C.; Mark, A. E. An Automated Force Field Topology Builder (ATB) and Repository: Version 1.0. *J. Chem. Theory Comput.* **2011**, *7*, 4026−4037.
(66) Koziara, K. B.; Stroet, M.; Malde, A. K.; Mark, A. E. Testing and Validation of the Automated Topology Builder (ATB) Version 2.0: Prediction of Hydration Free Enthalpies. *J. Comput.-Aided Mol. Des.* **2014**, *28*, 221−233.
(67) Stroet, M.; Caron, B.; Visscher, K. M.; Geerke, D. P.; Malde, A. K.; Mark, A. E. Automated Topology Builder Version 3.0: Prediction of Solvation Free Enthalpies in Water and Hexane. *J. Chem. Theory Comput.* **2018**, *14*, 5834−5845.
(68) Berendsen, H. J. C.; Postma, J. P. M.; van Gunsteren, W. F.; Hermans, J. Interaction Models for Water in Relation to Protein Hydration. In: *Intermolecular Forces. The Jerusalem Symposia on Quantum Chemistry and Biochemistry*; Pullman, B. Ed.; Springer, Dordrecht, 1981, pp. 331−342.
(69) Humphrey, W.; Dalke, A.; Schulten, K. VMD: Visual Molecular Dynamics. *J. Mol. Graph.* **1996**, *14*, 33−38.
(70) Stone, J. E.; University of Missouri-Rolla. Graduate School. *An Efficient Library for Parallel Ray Tracing and Animation: A Thesis Presented to the Faculty of the Graduate School of the University of Missouri-Rolla in Partial Fulfillment of Requirements for the Degree of Master of Science in Computer Science*; 1998.
(71) Leach, A. R.. *Molecular Modelling: Principles and Applications,* 2nd ed; Pearson Education: Harlow , 2001.
(72) Basu, S.; Mukharjee, D. Salt-Bridge Networks within Globular and Disordered Proteins: Characterizing Trends for Designable Interactions. *J. Mol. Model.* **2017**, *23*, 206.
(73) Donald, J. E.; Kulp, D. W.; DeGrado, W. F. Salt Bridges: Geometrically Specific. *Designable Interactions. Proteins* **2011**, *79*, 898−915.

https://doi.org/10.1021/acsomega.1c01744
ACS Omega 2021, 6, 15382−15391